Finance Research Letters 85 (2025) 108120

Contents lists available at ScienceDirect

Finance Research Letters

journal homepage: www.elsevier.com/locate/frl

Option pricing with a two-piece lognormal distribution

M. Magdalena Vich-Llompart [a], Luiz Vitiello [b,*]

[a] Department of Business Management & Department of International Studies, Washington College, 300 Washington Avenue, 21620 Chestertown, MD, USA

[b] Essex Business School, University of Essex, Wivenhoe Park, Colchester, CO4 3SQ, UK

ARTICLE INFO

JEL classification:
C63
G12
G13

Keywords:
Two-piece lognormal distribution
Split distribution
Option pricing
Illiquid underlying asset

ABSTRACT

We derive a closed-form European option pricing model in a discrete-time utility-based setting where the underlying asset has a two-piece lognormal distribution. In our set-up, the market does not have to be dynamically complete, which makes our model applicable even in cases in which the underlying asset is illiquid. The two-piece lognormal distribution results from joining two opposite halves of two distinct lognormal distributions, where each half has a different scale parameter. Hence, it is possible to adjust the tails of the distributions to accommodate the implied volatility of in-the-money and out-of-the-money options. We show that our option pricing equation can generate several types of volatility patterns and therefore can be used to price a wide range of assets.

1. Introduction

We derive an European option pricing model based on a two-piece lognormal distribution in a discrete-time utility-based framework. In this set-up, the market does not have to be dynamically complete, making it possible to apply our option pricing equation even in cases in which the underlying asset is illiquid.[1] As our model can capture different volatility patterns, it can be used to price a wide range of assets. We show that our model can produce volatility patterns often observed in commodities, equities, oil markets, among others.

The two-piece lognormal distribution, also known as split lognormal distribution, arises from joining two opposite halves of two distinct lognormal distributions, where the two halves have the same location parameter but different scale parameters. Therefore, it makes it possible to separately adjust the volatility of each tail of the distribution. This is a particular important feature for the pricing of options, as the tails of the distributions can be adjusted to accommodate the implied volatility of in-the-money and out-of-the-money options.

Introduced by Fechner (1897), the two-piece normal distribution had a tumultuous history having been rediscovered many times along the years.[2] Nevertheless, it has been applied to many different areas of knowledge. In finance and economics its popularity increased considerably when the Bank of England started using it in its inflation report (Britton et al. (1998)). In addition to applications to inflation forecast (Blix and Sellin (1998, 2000), Banerjee and Das (2011)), the two-piece normal distribution has also been applied to foreign currency futures by Pan et al. (1995), to value at risk, expected shortfall, portfolio weights, and asset

* Corresponding author.
E-mail addresses: mvich2@washcoll.edu (M.M. Vich-Llompart), lrviti@essex.ac.uk (L. Vitiello).

[1] Brennan (1979), for instance, provides several examples of illiquid assets that can be priced using discrete-time, utility-based models. These include certain types of tax liability, the value of income bonds, costs that will be incurred only in the event of bankruptcy, and options to purchase physical assets at the maturity of a lease contract. In all of these examples, either the contingent claim, or the underlying asset, or both are not traded.

[2] See Wallis (2014).

https://doi.org/10.1016/j.frl.2025.108120
Received 9 June 2025; Received in revised form 26 July 2025; Accepted 6 August 2025
Available online 14 August 2025

pricing by de Roon and Karehnke (2017a),[3] and to estimate and test skewness in stochastic volatility models by Lee and Kang (2023) to cite just some of its many applications.

The two-piece lognormal distribution can be obtained from a simple transformation of the two-piece normal distribution. However, while the two-piece normal distribution has been applied to finance and economics, it seems its lognormal counterpart has not.[4] Our paper aims to address this gap in the existing literature by introducing the two-piece lognormal distribution as a novel approach to asset valuation.

The two-piece option pricing model developed here is obtained in closed-from solution, it does not depend on the expected values of consumption and of the underlying asset; it only depends on their volatilities and correlation. The Black and Scholes (1973) is a special case of ours. We show that our two-piece lognormally-distributed option pricing model can capture volatility skews, which is likely to be one of the most common volatility patterns observed in financial markets.[5]

This paper is divided as follows: Section 2 introduces the distributional assumptions. In Section 3 we obtain relevant equilibrium market relationships, and in Section 4 we derive a two-piece lognormal option pricing model. In Section 5 we present the results of a simple empirical exercise using market data. Section 6 concludes.

2. The two-piece lognormal distribution

This section introduces the distributional assumptions. We start with the two-piece lognormal distribution, defined below.

Definition 1 (*the two-piece lognormal distribution*)**.** A variable x is said to have a two-piece lognormal distribution, $x \sim TP\Lambda\left(\mu_x, \sigma_x, \theta\right)$, if its density is given by

$$f_{TP\Lambda}(x) = \begin{cases} A \exp\left[-\frac{1}{2\sigma_x^2}\left(\ln x - \mu_x\right)^2\right] & x \leq \exp\left(\mu_x\right) \\ A \exp\left[-\frac{1}{2\theta\sigma_x^2}\left(\ln x - \mu_x\right)^2\right] & x > \exp\left(\mu_x\right), \end{cases} \tag{1}$$

where μ_x is the location parameter, $\sigma_x > 0$ is the scale parameter, $\theta > 0$ is the skewness parameter, and $A = (2/\pi)^{1/2}\left((1+\theta)\, x\sigma_x\right)^{-1}$.

The role of θ in Eq. (1) can be summarized as follows: if $\theta > 1$ the resulting distribution will have a thinner left tail and a heavier right tail than the lognormal distribution. For $\theta < 1$ the resulting distribution will have a heavier left tail and a thinner right tail than the lognormal distribution, and for $\theta = 1$ the resulting distribution is lognormal (see Villani and Larsson (2006)). An example of the two-piece lognormal density for $\mu_z = 0.1$, $\sigma_x = 0.5$, and $\theta = 0.5, 1, 1.4$ is presented in Fig. 1.

Definition 2 (*the two-piece lognormal–lognormal bivariate distribution*)**.** Variables x and w are said to have a two-piece lognormal–lognormal bivariate distribution, $(x, w) \sim TP\Lambda - \Lambda\left(\mu_x, \mu_w, \sigma_x, \sigma_w, \theta, \rho\right)$ if

$$f_{TP\Lambda-\Lambda}(x, w) = \begin{cases} \frac{A}{\sigma_w w\sqrt{2\pi}\sqrt{(1-\rho^2)}} \exp\left[-\frac{1}{2(1-\rho^2)}\left(B^2 + C^2 - 2\rho BC\right)\right] & x \leq \exp\left(\mu_x\right) \\ \frac{A}{\sigma_w w\sqrt{2\pi}\sqrt{(1-\rho^2)}} \exp\left[-\frac{1}{2(1-\rho^2)}\left(B^2 + \theta^{-2}C^2 - 2\rho\theta^{-1}BC\right)\right] & x > \exp\left(\mu_x\right), \end{cases} \tag{2}$$

where $B = \left(\ln w - \mu_w\right)/\sigma_w$, $C = \left(\ln x - \mu_x\right)/\sigma_x$, ρ is the correlation coefficient, and A is as in Definition 1.

The univariate distribution in Eq. (1) and the bivariate distribution in Eq. (2) can be obtained by a simple transformation from the normal distribution (see Johnson (1949a,b) and Blix and Sellin (2000)).[6] An important feature of Eq. (2) is that while x has a two-piece marginal density, the marginal density of w is not lognormal.[7] Each half of the two-piece distribution can be seen as a form of truncated distribution. As x and w are correlated, Arnold et al. (1993) show that in a bivariate normal-truncated-normal distribution, the non-truncated marginal distribution is not normal. This result can be generalized to the bivariate lognormal-truncated-lognormal distribution and to the bivariate two-piece-lognormal–lognormal distribution.

[3] de Roon and Karehnke (2017a) claim to have introduced the two-piece normal distribution. Later, de Roon and Karehnke (2017b) correctly attribute it to Fechner (1897).

[4] To the best of our knowledge, there are no applications of the two-piece lognormal distribution to finance or economics. In contrast, the lognormal distribution has been widely used in composite distributions (sometimes also called split distributions). See for instance Scollnik (2007), and Grün and Miljkovic (2019).

[5] Wang et al. (2024), for instance, show that Gold prices are left skewed while the US dollar is right skewed.

[6] A multivariate two-piece lognormal distribution is proposed by Shah and Bhavsar (2014). However, the authors do not provide details of how the multivariate distribution was constructed.

[7] As demonstrated in the following sections, knowledge of the marginal density of w is not a requirement for our results. Brennan (1979) and Câmara (2003) show that the bivariate distribution of the underlying asset and wealth is a sufficient distributional condition to derive an option pricing equation.

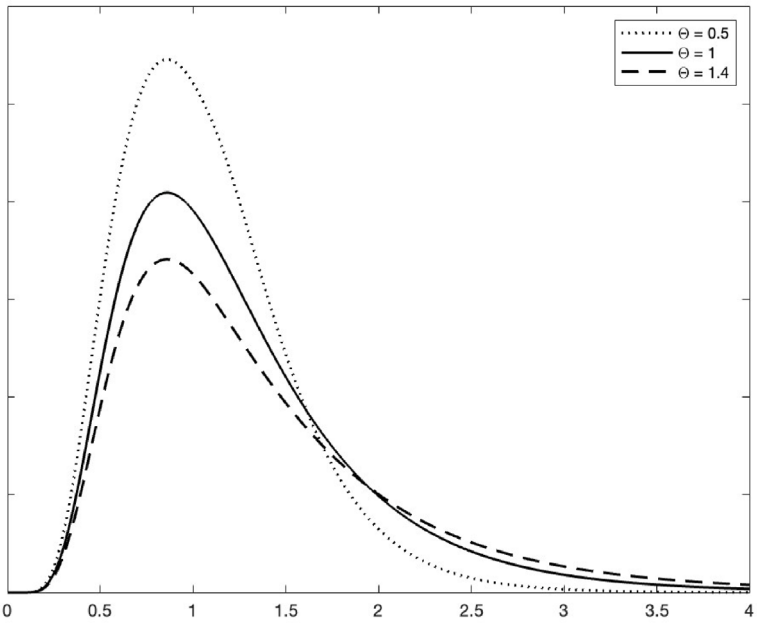

Fig. 1. The two-piece lognormal density. Example of a two-piece lognormal density of z in Eq. (1) with $\mu_z = 0.1$, $\sigma_z = 0.5$, and different values of θ.

3. Market equilibrium relationships

We follow an economy similar to Brennan (1979), where a representative investor with a standard power utility function faces the problem of maximizing her expected utility function of consumption. This setting does not require the continuous rebalancing of a risk-free portfolio, which can be useful for pricing options on illiquid assets.

The solution to the problem faced by the investor leads to the equilibrium stock return and to the equilibrium riskless bond price, represented respectively by the following two Euler equations,

$$1 = E\left[\left(\frac{C}{C_0}\right)^{-y}\frac{z}{z_0}\right], \tag{3}$$

$$\exp(-r) = E\left[\left(\frac{C}{C_0}\right)^{-y}\right], \tag{4}$$

where y is the risk aversion parameter, C_0 is consumption at time 0 ($t = 0$), C is terminal consumption, z_0 is the stock price at time 0, z is the terminal stock price, r is the risk-free rate over period t, t is a period of time in years, and $\exp(-r)$ is the current price of a riskless bond that pays \$1 at maturity.

Definition 3 (*the distribution of the underlying asset price and consumption*)**.** The gross return z/z_0 has a two-piece lognormal distribution as in Definition 1, and z/z_0 and C/C_0 have a two-piece lognormal–lognormal bivariate distribution as in Definition 2.

With the distributional assumptions in place, we can obtain the market equilibrium relationships for the underlying asset and bond, which are presented in the following two propositions.

Proposition 4. *(The market equilibrium price of the bond) Assume that the equilibrium relationship in Eq. (4) holds, and that consumption has a distribution as in Definition 3. Then the market equilibrium price of a riskless bond is given by*

$$\exp(-r) = 2(1+\theta)^{-1}\left(N\left(y\rho\sigma_C\right) + \theta N\left(-y\rho\sigma_C\right)\right)\exp\left(\frac{1}{2}y^2\sigma_C^2 - y\mu_C\right), \tag{5}$$

where $N(\cdot)$ is the cumulative distribution function of a standard normal random variable.

Proof. See Appendix. ■

Eq. (5) can be split in two parts: the expression in the exponent is equivalent to the equilibrium relationship for a lognormally distributed random variable. The rest of the equation can be regarded as an adjustment for the two-piece distribution. By letting $\theta = 1$ it is easy to verify that the first part cancels out and we are left with only the exponent part.

Proposition 5 (*the market equilibrium underlying asset return*). *Assume that the equilibrium relationship in Eq. (3) holds and that* z/z_0 *has a distribution as in Definition 3. Then the market equilibrium return for the underlying asset is given by*

$$1 = \frac{2e^{\frac{1}{2}y^2\sigma_C^2}}{1+\theta}\left[\exp\left(\mu_z - y\left(\mu_C + \rho\sigma_C\sigma_z\right) + 0.5\sigma_z^2\right) N\left(y\rho\sigma_C - \sigma_z\right)\right.$$
$$\left. + \ \theta\exp\left(\mu_z - y\left(\mu_C + \theta\rho\sigma_C\sigma_z\right) + 0.5\theta^2\sigma_z^2\right) N\left(\theta\sigma_z - y\rho\sigma_C\right)\right]. \tag{6}$$

Proof. See Appendix. ■

As with Eq. (5), the equation above also collapses into the standard lognormal equilibrium underlying asset return when $\theta = 1$.

4. The two-piece lognormal option pricing equation

Here we obtain the price of an option written on an underlying asset z. As in Eq. (3) and (4), the Euler equation for the price of an option is given by

$$v = E\left[\left(C/C_0\right)^{-y} h\left(v\right)\right], \tag{7}$$

where $h(v)$ is the payoff of the option.

In Proposition 6 we derive the equation for a call option based on the two-piece lognormal distribution, where $h(v) = \max(z-k,0)$ and k is the strike price.[8] The equation for a put option with payoff $\max(k-z,0)$ can be easily obtained by following similar steps.

Proposition 6 (*the call option equation*). *Assume that Propositions 4 and 5 hold. Then the price of a call option written on* z *is given by*

$$v = \frac{z_0}{Q_1}\theta\exp\left(\left(1-\theta\right)y\rho\sigma_C\sigma_z - \frac{1}{2}\left(1-\theta^2\right)\sigma_z^2\right) N\left(\min\left(\frac{\delta}{\theta},0\right) + \theta\sigma_z - y\rho\sigma_C\right)$$
$$+ \ \frac{z_0}{Q_1}\left[N\left(\max\left(\delta,0\right) + \sigma_z - y\rho\sigma_C\right) - N\left(\sigma_z - y\rho\sigma_C\right)\right]$$
$$- \ \frac{ke^{-r}}{Q_2}\left[\theta N\left(\min\left(\frac{\delta}{\theta},0\right) - y\rho\sigma_C\right) + N\left(\max\left(\delta,0\right) - y\rho\sigma_C\right) - N\left(-y\rho\sigma_C\right)\right], \tag{8}$$

where

$$Q_1 = \theta\exp\left(\left(1-\theta\right)y\rho\sigma_C\sigma_z - \frac{1}{2}\left(1-\theta^2\right)\sigma_z^2\right) N\left(\theta\sigma_z - y\rho\sigma_C\right) + N\left(y\rho\sigma_C - \sigma_z\right),$$

$$Q_2 = N\left(y\rho\sigma_C\right) + \theta N\left(-y\rho\sigma_C\right),$$

$$\delta = \frac{1}{\sigma_z}\left(\ln\frac{z_0 Q_2}{kQ_1} + y\rho\sigma_C\sigma_z + r - \frac{\sigma_z^2}{2}\right).$$

Proof. See Appendix. ■

Figs. 2 and 3 depict some of the volatility patterns that can be obtained from simulated prices generated from Eq. (8), with $\sigma_z = 0.3$, $\sigma_C = 0.1$, $r = 0.1$, $\rho = 0.8$, $y = 2$, and different values of θ. To obtain these implied volatility patterns, we search, for each strike price, for a volatility (the implied volatility) that makes the Black and Scholes price equal to the two-piece lognormal option pricing model price. The volatility patterns shown in both figures are standardized by the volatility of the at-the-money option.

In Fig. 2, $\theta \geq 1$, leading to an implied volatility that increases in k, and as θ increases, the curve rotates anti-clockwise. This volatility pattern has been observed in oil markets, agricultural commodities and VIX, among others (see Zhou (1998), Soini and Lorentzen (2019), Yoon et al. (2022)).

In Fig. 3, $\theta \leq 1$, leading to an implied volatility that decreases in k, and as θ decreases the curve rotates clockwise. This pattern is the standard pattern for equity options and many classes of assets (see for instance Rubinstein (1994)).

4.1. Special cases

There are two special cases of Eq. (8) that are worth mentioning. The first one is when we set $y = 0$ in Eq. (8), which is equivalent to risk neutrality. The risk-neutral two-piece option pricing equation is given by

$$v = \frac{z_0}{Q_1}\theta\exp\left(-\frac{1}{2}\left(1-\theta^2\right)\sigma_z^2\right) N\left(\min\left(\frac{\delta}{\theta},0\right) + \theta\sigma_z\right) + \frac{z_0}{Q_1}\left[N\left(\max\left(\delta,0\right) + \sigma_z\right) - N\left(\sigma_z\right)\right]$$
$$- \ \frac{ke^{-r}}{0.5\left(1+\theta\right)}\left[\theta N\left(\min\left(\frac{\delta}{\theta},0\right)\right) + N\left(\max\left(\delta,0\right)\right) - 0.5\right], \tag{9}$$

[8] Note that the location parameters μ_C and μ_z are not present in Eq. (8).

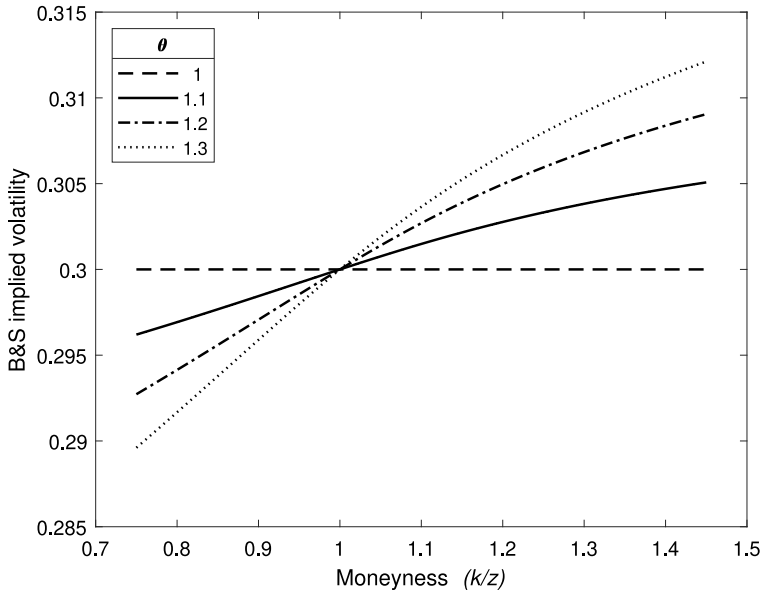

Fig. 2. Implied volatilities with $\theta \geq 1$. Volatility patterns obtained from Eq. (8) with $\sigma_z = 0.3$, $\sigma_C = 0.1$, $r = 0.1$, $\rho = 0.8$, $y = 2$, and different values of θ.

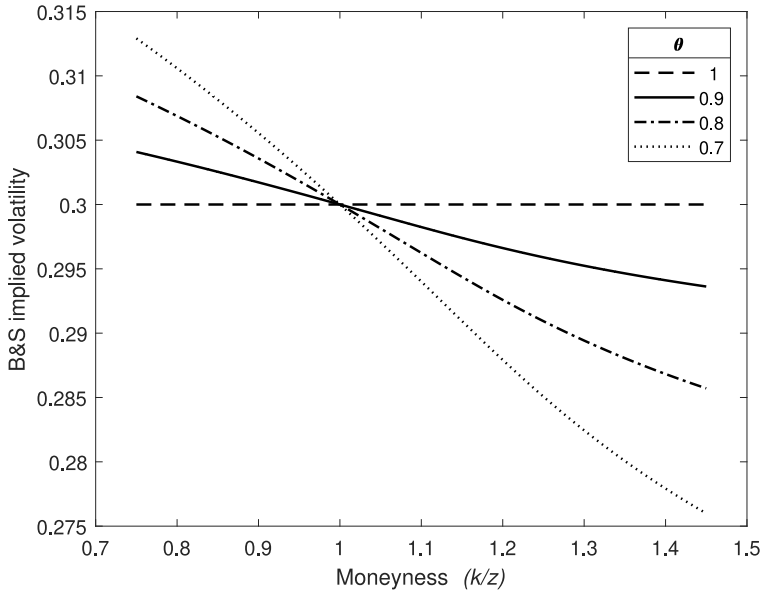

Fig. 3. Implied volatilities with $\theta \leq 1$. Volatility patterns obtained from Eq. (8) with $\sigma_z = 0.3$, $\sigma_C = 0.1$, $r = 0.1$, $\rho = 0.8$, $y = 2$, and different values of θ.

where

$$Q_1 = \theta \exp\left(-\frac{1}{2}\left(1-\theta^2\right)\sigma_z^2\right) N\left(\theta\sigma_z\right) + N\left(-\sigma_z\right),$$

$$\delta = \frac{1}{\sigma_z}\left(\ln\frac{0.5 z_0 (1+\theta)}{k Q_1} + r - \frac{\sigma_z^2}{2}\right).$$

The second case is when, in addition to $y = 0$, we let $\theta = 1$. This is equivalent to risk-neutrality and a lognormally distributed underlying asset price. The resulting equation is equivalent to the Black and Scholes (1973) equation.

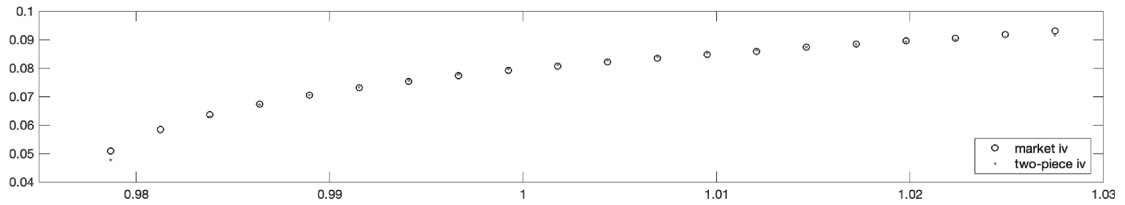

Fig. 4. Market and model implied volatility patterns for Gold.
Implied volatility pattern obtained from call options on Gold futures on September 8, 2023 with 48 days to maturity. The graph compares the implied volatility patterns obtained from the observed market prices (*market iv*) with those obtained using the two-piece option pricing model (*two-piece iv*) in Eq. (8) with $\hat{\sigma}_z = 8.75\%$ p.a. and $\hat{\theta} = 1.296$.

5. Empirical application

In this section we evaluate the performance of the two-piece option pricing model. In Section 5.1 we show how the two-piece model fits the observed market option prices. In Section 5.2, we compare the two-piece model against two well-known option pricing models.

5.1. Model fitting

We provide a simple empirical application where we use our two-piece lognormal option pricing model to fit the implied volatility of call options on Gold (100 oz) futures contracts and on the S&P500 index.

For Gold, we collected call options on September 8, 2023 with 48 days to maturity and when the futures contract price (the underlying asset) was 1,946.50 USD. For the S&P500 index, we use call options on May 13, 2024 with 18 days to maturity with a S&P500 spot index value of 5,225.77 USD. Data was collected from Bloomberg.

To apply our model we use the bid–ask mid-point option prices, and we work with a moneyness range (k/S) of 0.97–1.03.[9] The risk-free rate (r) used is 4.09% p.a.,[10] and the risk aversion value (y) is taken from the risk aversion index by Bekaert et al. (2022).[11] The values used are 2.72 for Gold and 2.59 for the S&P500. For ρ and σ_C we use 0.9 and 15% p.a., respectively.[12]

To produce the two-piece option pricing model implied volatilities, we first consider all options written on the same underlying and with the same time to maturity available on a specific day. We then search for the value of the parameters σ_z and θ that minimize the square distance between observed and model prices. Finally, we use these estimated values ($\hat{\sigma}_z$ and $\hat{\theta}$) to calculate the option prices for each strike using Eq. (8).[13] For Gold, we apply first the arbitrage-free condition $F = Se^{rt}$. Finally we search for the Black and Scholes (1973) implied volatility for each strike.[14]

The estimated values of the two-piece option pricing model parameters for Gold are $\hat{\sigma}_z = 8.75\%$ p.a. and $\hat{\theta} = 1.296$. As $\hat{\theta} > 1$, the implied volatilities are an increasing function of the strike price. The two-piece implied volatility pattern for Gold is shown in Fig. 4, alongside the market (Black and Scholes) implied volatilities (*market iv*). As can be seen, both the two-piece and the market implied volatilities fall very close together, concluding that the two-piece option pricing model provides an excellent fit to the market data.

Fig. 5 depicts the two-piece lognormal density corresponding to the implied volatility pattern shown in Fig. 4 together with its lognormal counterpart. We can see that the two-piece lognormal density has a heavier right tail and a lower mode, which confirms that an option pricing model based only on a simple lognormal distribution, such as the Black and Scholes (1973) and Black (1976) models, cannot capture this level of skewness.

For the S&P500, the estimated values are $\hat{\sigma}_z = 0.14\%$ p.a. and $\hat{\theta} = 0.499$. As $\hat{\theta} < 1$ the implied volatilities are a decreasing function of the strike price. Fig. 6 shows the market and the two-piece implied volatility patterns for options on the S&P500 index. Once again, the figure reveals a good fit of our two-piece option pricing model to the observed implied volatility. Fig. 7 depicts the corresponding two-piece lognormal density together with its lognormal counterpart for the S&P500 index. This figure shows how the two-piece lognormal distribution has a heavier left tail. Results for the S&P500 index are in line with the existing literature which claims that the distribution of asset returns is left skewed and leptokurtic, see, for instance, Jackwerth and Rubinstein (1996) and Jackwerth (2004).

[9] Options within this range are more liquid, containing therefore more reliable information. See for instance Jackwerth (2000).

[10] During the dates considered in this analysis, the 10-year Treasury rates fluctuate around 4%.

[11] https://www.nancyxu.net/risk-aversion-index

[12] As a robustness check, we conduct a sensitivity analysis using different values of ρ and σ_C. The results obtained are similar and do not change the shape of the implied distribution. For instance, keeping $\sigma_C = 0.15\%$ while changing ρ from 0.9 to 0.2 results in a change in the IVRMSE (see next subsection) of approximately 3.4% for the S&P500 and 1.2% for Gold. Similarly, keeping $\rho = 0.9$ and changing σ_C from 15% to 5% leads to a change in the IVRMSE of approximately 3% for the S&P500 and 1.1% for Gold.

[13] Considering the short maturity of our options, we ignore extra costs related to the price of futures contracts, such as convenience yield and storage costs.

[14] See for instance Mayhew (1995).

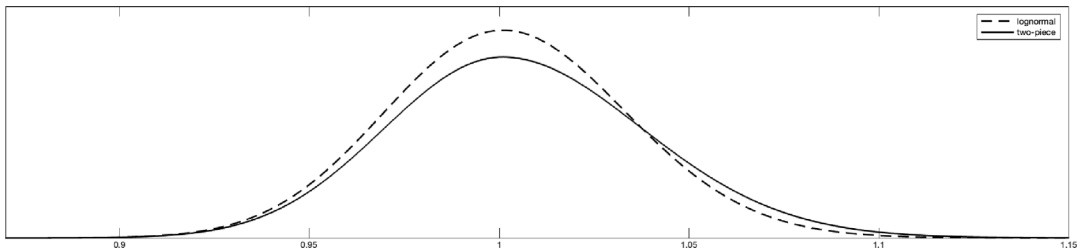

Fig. 5. Implied density for Gold.
The graph compares the two-piece density ($two-piece$) equivalent to the implied volatility pattern obtained from the two-piece option pricing model in Eq. (8), and its lognormal counterpart ($lognormal$). The data used are call prices for options on Gold on September 8, 2023 with 48 days to maturity.

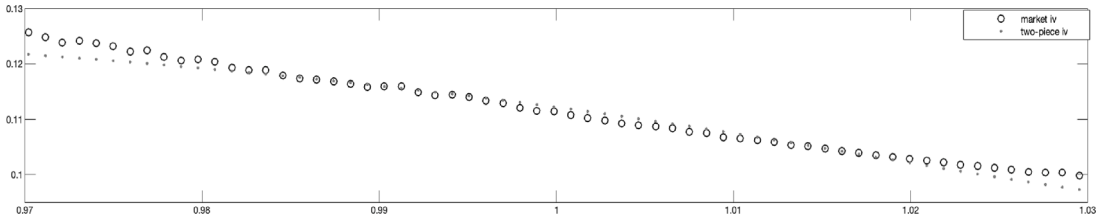

Fig. 6. Market and model implied volatility patterns for the S&P500.
Implied volatility pattern obtained from call options on the S&P500 on May 13, 2024 with 18 days to maturity. The graph compares the implied volatility patterns obtained from the observed market prices (*market iv*) with those obtained using the two-piece option pricing model (*two-piece iv*) in Eq. (8) with $\hat{\sigma}_z = 0.14\%$ p.a. and $\hat{\theta} = 0.499$.

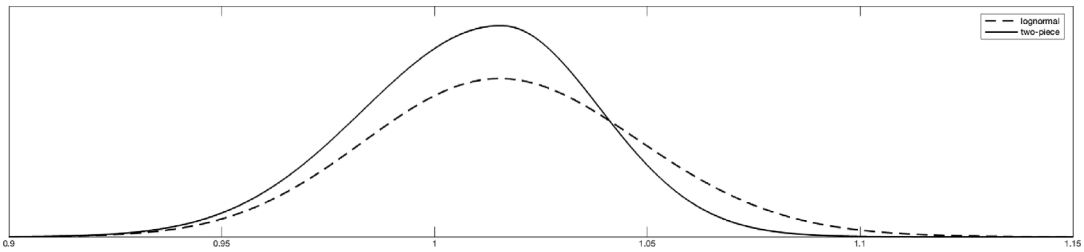

Fig. 7. Implied density for S&P500.
The graph compares the two-piece density ($two-piece$) equivalent to the implied volatility pattern obtained from the two-piece option pricing model in Eq. (8), and its lognormal counterpart ($lognormal$). The data used are call prices for options on the S&P500 on May 13, 2024 with 18 days to maturity.

5.2. Model performance

Here, we compare the performance of the two-piece model against two well-known option pricing models: the jump-diffusion model (Merton (1976)), and the stochastic volatility model (Heston (1993)).

We assess the goodness of fit of these models using the implied volatility root mean squared error (IVRMSE) proposed by Christoffersen and Jacobs (2004) which is based on the discrepancies between the observed volatility and those implied by each one of the models, as follows:

$$IVRMSE(j) = \sqrt{\frac{1}{N}\sum_{i=1}^{N}(\sigma_i - \hat{\sigma}_{i,j})^2}, \tag{10}$$

where σ_i is the market implied volatility, and $\hat{\sigma}_{i,j}$ is the implied volatility from model j for all i observations on a given day.

We use options written on the S&P500 index, Gold, and Crude Oil across two different maturities for each underlying asset. To ensure that the two-piece model is comparable to the other models, we use its risk-neutral version as presented in Eq. (9), which requires the estimation of only two parameters: σ_z and θ. Since the jump-diffusion model (JD hereafter) and the stochastic volatility model (SV hereafter) require the estimation of four and five parameters, respectively, we reduce the dimensionality of the optimization problem by setting the volatility of the underlying asset to be the same for all models. The other model-related parameters are estimated implicitly i.e. the parameters are selected to minimize the sum of the square differences between observed and model prices.

Table 1
Implied volatility root mean squared errors (IVRMSE) for the S&P500 index, Gold, and Crude Oil across different maturities, τ. (IVRMSE x1000).

Moneyness	Asset	2-piece (RN)	JD	SV
Whole sample	S&P500 (τ = 18)	**3.40**	56.12	13.37
	S&P500 (τ = 39)	**3.73**	91.12	19.94
	Gold (τ = 48)	3.08	6.84	**2.06**
	Gold (τ = 31)	6.47	26.24	**3.35**
	Crude Oil (τ =7)	**74.04**	110.46	159.91
	Crude Oil (τ =39)	**9.39**	152.63	26.47
Moneyness <1	S&P500 (τ = 18)	**3.66**	50.23	16.64
	S&P500 (τ = 39)	**5.06**	85.03	18.24
	Gold (τ = 48)	2.80	8.35	**2.44**
	Gold (τ = 31)	7.40	24.80	**4.30**
	Crude Oil (τ =7)	**61.94**	126.57	190.60
	Crude Oil (τ =39)	**9.35**	159.32	49.65
Moneyness >1	S&P500 (τ = 18)	**3.25**	59.17	11.12
	S&P500 (τ = 39)	**2.68**	94.46	20.86
	Gold (τ = 48)	3.09	6.72	**2.03**
	Gold (τ = 31)	5.52	27.44	**2.18**
	Crude Oil (τ =7)	**83.93**	92.60	123.90
	Crude Oil (τ =39)	9.40	150.12	**7.70**
Moneyness >1.03	S&P500 (τ = 18)	**5.34**	65.27	8.73
	S&P500 (τ = 39)	**3.71**	99.23	19.07
	Gold (τ = 48)	4.12	8.03	**2.64**
	Gold (τ = 31)	8.58	37.42	**3.28**
	Crude Oil (τ =7)	104.00	100.19	**96.27**
	Crude Oil (τ =39)	11.06	150.25	**8.41**

This table reports the values of the IVRMSE loss function for the risk-neutral two-piece option pricing model (2-piece (RN)) obtained from Eq. (8), as well as Merton's jump-diffusion model (JD), and Heston stochastic volatility model (SV). τ represents the time to maturity. The data sample consists of all available call options on the S&P500 (collected on October 27, 2023 and May 13, 2024 for those options with τ = 31 and τ= 48 days, respectively), as well as Gold and Crude Oil, all of which were collected on September 8, 2023. Values in bold indicate the lowest IVRMSE for each row.

The next step is to use the estimated parameters to obtained the model prices, which are then used as an input to the Black and Scholes (1973) model to obtain the corresponding implied volatility. These are the implied volatilities used in the calculation of the IVRMSE.

Table 1 reports the values of the IVRMSE for the two-piece, JD, and SV option pricing models for the S&P500 index, Gold, and Crude Oil for different levels of Moneyness. The first row, for instance, shows the results for the S&P500 index with options maturing in 18 days (τ). In this case, the two-piece model has the smallest IVRMSE, suggesting a superior fitting when compared to the other models.

The results in Table 1 suggest that the two-piece model performs better for the S&P500 and Crude Oil, while the SV model shows superior performance for Gold. However, as the analysis shifts toward out-of-the-money and deep out-of-the-money options (Moneyness > 1 and Moneyness > 1.03, respectively), the performance of the SV model improves, particularly for Crude Oil.

It is important to highlight, that this is an in-sample fitting test. In general, more complex models tend to provide a better in-sample fit but do not necessarily guarantee a better out-of-sample performance due to overfitting. That is, while the in-sample performance of the two-piece model is comparable to that of the SV model, the former requires the estimation of only two parameters whereas the latter requires the estimation of five.

6. Conclusion

Based on a two-piece lognormal distribution, we derive an option pricing model in a utility-based framework. Our model is derived in a discrete-time setting and is capable of pricing options even when the underlying asset is illiquid, since it does not require markets to be dynamically complete. As the two-piece lognormal distribution can capture positive and negative levels of skewness, our model can generate several types of volatility patterns observed in different types of assets which makes it a particular interesting tool to price a wide range of different types of assets such as equities or commodities, among others. This is demonstrated through an empirical application using call option market data on Gold, Crude Oil and the S&P500 index.

Finally, considering the Bank of England's use of the two-piece distribution in its inflation report, an interesting future application would be to extend the model presented here to the pricing of inflation derivatives.

CRediT authorship contribution statement

M. Magdalena Vich-Llompart: Writing – review & editing, Writing – original draft, Validation, Software, Formal analysis. **Luiz Vitiello:** Writing – review & editing, Writing – original draft, Validation, Project administration, Methodology, Conceptualization.

Declaration of competing interest

The authors have no conflicts of interest to disclose, and they confirm that this work is original, has not been published elsewhere, and is not currently under consideration for publication elsewhere.

Appendix

Proof (*Proposition* 4)**.** Given Eq. (4) and considering definitions 2 and 3, the equilibrium price of a bond can be obtained by solving

$$e^{-r} = \int \int \left(C/C_0\right)^{-y} f_{TPA-A}\left(z, C\right) dC dz. \tag{A.1}$$

Changing variables, simplifying, and evaluating the remaining expression yields Eq. (5). ■

Proof (*Proposition* 5)**.** Given Eq. (3) and considering definitions 2 and 3, the equilibrium underlying asset return can be obtained by solving

$$1 = \int \int \left(C/C_0\right)^{-y} z/z_0 f_{TPA-A}\left(z, C\right) dC dz. \tag{A.2}$$

Changing variables, evaluating the remaining expression for C and simplifying leads to the following equation

$$1 = \frac{2e^{\mu_z - y\mu_C + 0.5y^2\sigma_C^2}}{(1+\theta)\sqrt{2\pi}} \left(\int_{-\infty}^{0} e^{0.5\sigma_z^2 - y\rho\sigma_z\sigma_C} e^{-0.5\left(z + y\rho\sigma_C - \sigma_z\right)^2} dz + \int_{0}^{\infty} e^{0.5\theta^2\sigma_z^2 - \theta y\rho\sigma_z\sigma_C} e^{-0.5\left(z + y\rho\sigma_C - \theta\sigma_z\right)^2} \right). \tag{A.3}$$

Finally, evaluating the above expression yields Eq. (6). ■

Proof (*Proposition* 6)**.** Given Eq. (7) and considering definitions 2 and 3, the price of a call option can be obtained by solving $1 = \int \int \left(C/C_0\right)^{-y} h\left(v\right) f_{TPA-A}\left(z, C\right) dC dz$. Changing variables, evaluating the remaining expression for C and z, and simplifying leads to the following equation

$$\begin{aligned} v = {} & \frac{2z_0 e^{\mu_z + 0.5y^2\sigma_C^2 - y\mu_C}}{1+\theta} \left[\theta e^{0.5\theta^2\sigma_z^2 - \theta y\rho\sigma_z\sigma_C} N\left(\min\left(\frac{d}{\theta}, 0\right) + \theta\sigma_z - y\rho\sigma_C\right) \right. \\ & \left. + e^{0.5\sigma_z^2 - y\rho\sigma_z\sigma_C} \left(N\left(\max\left(d, 0\right) + \sigma_z - y\rho\sigma_C\right) - N\left(\sigma_z - y\rho\sigma_C\right)\right) \right] \\ & - \frac{2ke^{0.5y^2\sigma_C^2 - y\mu_C}}{1+\theta} \left[N\left(\max\left(d, 0\right) - y\rho\sigma_C\right) + \theta N\left(\min\left(\frac{d}{\theta}, 0\right) - y\rho\sigma_C\right) - N\left(-y\rho\sigma_C\right) \right], \end{aligned} \tag{A.4}$$

where $d = \left(\ln\left(z_0/k\right) + \mu_z\right)/\sigma_z$.

Solving Eq. (5) and (6) for μ_C and μ_z respectively, substituting them into the above expression and simplifying yields Eq. (8). ■

Data availability

The authors do not have permission to share data.

References

Arnold, B., Beaver, R., Groeneveld, R., Meeker, W., 1993. The nontruncated marginal of a truncated bivariate normal distribution. Psychometrika 58, 471–488. http://dx.doi.org/10.1007/BF02294652.

Banerjee, N., Das, A., 2011. Fan chart: methodology and its application to inflation forecasting in India. Reserv. Bank India Work. Pap. Ser. 5/ 2011.

Bekaert, G., Engstrom, E., Xu, N., 2022. The time variation in risk appetite and uncertainty. Manag. Sci. 68, 3975–4004. http://dx.doi.org/10.1287/mnsc.2021.4068.

Black, F., 1976. The pricing of commodity contracts. J. Financ. Econ. 3, 167–179. http://dx.doi.org/10.1016/0304-405X(76)90024-6.

Black, F., Scholes, M., 1973. The pricing of options and corporate liabilities. J. Political Econ. 81, 637–654. http://dx.doi.org/10.1086/260062.

Blix, M., Sellin, P., 1998. Uncertainty bands for inflation forecasts. Sveriges Riksbank Work. Pap. Ser. 65.

Blix, M., Sellin, P., 2000. A bivariate distribution for inflation and output forecasts. Sveriges Riksbank Work. Pap. Ser. 102.

Brennan, M., 1979. The pricing of contingent claims in discrete time models. J. Financ. 34, 53–68. http://dx.doi.org/10.1111/j.1540-6261.1979.tb02070.x.

Britton, E., P., F., J., W., 1998. The inflation report projections: understanding the fan chart. Bank Engl. Q. Bull. 38:1, 30–37.

Câmara, A., 2003. A generalization of the brennan-rubinstein approach for the pricing of derivatives. J. Financ. 58 (2), 805–819. http://dx.doi.org/10.1111/1540-6261.00546.
Christoffersen, P., Jacobs, K., 2004. The importance of the loss function in option valuation. J. Financ. Econ. 72, 291–318. http://dx.doi.org/10.1016/j.jfineco.2003.02.001.
de Roon, F., Karehnke, P., 2017a. A simple skewed distribution with asset pricing applications. Rev. Financ. 21:6, 2169–2197. http://dx.doi.org/10.1093/rof/rfw040.
de Roon, F., Karehnke, P., 2017b. Addendum: a simple skewed distribution with asset pricing applications. Rev. Financ. 21:6, 2401. http://dx.doi.org/10.1093/rof/rfx049.
Fechner, G.T., 1897. Kollektivmasslehre. Engelmann, Leipz..
Grün, B., Miljkovic, T., 2019. Extending composite loss models using a general framework of advanced computational tools. Scand. Actuar. J. 8, 642–669. http://dx.doi.org/10.1080/03461238.2019.1596151.
Heston, S.L., 1993. A closed-form solution for options with stochastic volatility with applications to bond and currency options. Rev. Financ. Stud. (ISSN: 0893-9454) 6 (2), 327–343, DOI: 10.1016/0304-405X(76)90022-2.
Jackwerth, J.C., 2000. Recovering risk aversion from options prices and realized returns. Rev. Financ. Stud. 13, 433–451. http://dx.doi.org/10.1093/rfs/13.2.433.
Jackwerth, J.C., 2004. Option-Implied Risk-Neutral Distributions and Risk Aversion. The Ressearch Foundation of AIMR.
Jackwerth, J.C., Rubinstein, M., 1996. Recovering probability distributions from option prices. J. Financ. 51, http://dx.doi.org/10.1111/j.1540-6261.1996.tb05219.x.
Johnson, N.L., 1949a. Systems of frequency curves generated by methods of translation. Biometrika 36:1, 149–176. http://dx.doi.org/10.1093/biomet/36.1-2.149.
Johnson, N.L., 1949b. Bivariate distributions based on simple translation systems.. Biometrika 36:3, 297–304. http://dx.doi.org/10.2307/2332669.
Lee, C.W., Kang, K.H., 2023. Estimating and testing skewness in a stochastic volatility model. J. Empir. Financ. 72, 445–467. http://dx.doi.org/10.1016/j.jempfin.2023.04.009.
Mayhew, S., 1995. Implied volatility. Financ. Anal. J. 51:4, 8–20. http://dx.doi.org/10.2469/faj.v51.n4.1916.
Merton, R.C., 1976. Option pricing when underlying stock returns are discontinuous. J. Financ. Econ. (ISSN: 0304-405X) 3 (1), 125–144. http://dx.doi.org/10.1093/rfs/6.2.327.
Pan, M.S., Chan, K.C., Fok, C.W., 1995. The distribution of currency futures price changes: A two-piece mixture of normals approach. Int. Rev. Econ. Financ. 4:1, 69–78. http://dx.doi.org/10.1016/1059-0560(95)90056-X.
Rubinstein, M., 1994. Implied binomial trees. J. Financ. 49 (3), 771–818. http://dx.doi.org/10.1111/j.1540-6261.1994.tb00079.x.
Scollnik, D.P.M., 2007. On composite lognormal-Pareto models. Scand. Actuar. J. 1, 20–33. http://dx.doi.org/10.1080/03461230601110447.
Shah, P.B., Bhavsar, C.D., 2014. Two-piece multivariate lognormal distribution. Int. J. Sci.: Basic Appl. Res. 15:1, 164–170.
Soini, V., Lorentzen, S., 2019. Option prices and implied volatility in the crude oil market. Energy Econ. 83, 515–539. http://dx.doi.org/10.1016/j.eneco.2019.07.011.
Villani, M., Larsson, R., 2006. The multivariate split normal distribution and asymmetric principal components analysis. Comm. Statist. Theory Methods 35:6, 1123–1140. http://dx.doi.org/10.1080/03610920600672252.
Wallis, K.F., 2014. The two-piece normal, binormal, or double gaussian distribution: its origin and rediscoveries. Statist. Sci. 29:1, 106–112, http://www.jstor.org/stable/43288461.
Wang, M.-C., Chang, T., Mikhaylov, A., Linyu, J., 2024. A measure of quantile-on-quantile connectedness for the US treasury yield curve spread, the US dollar, and gold price. North Am. J. Econ. Financ. 74, 102232. http://dx.doi.org/10.1016/j.najef.2024.102232.
Yoon, J., Ruan, X., Zhang, J.E., 2022. VIX option-implied volatility slope and VIX futures returns. J. Futur. Mark. 42:6, 1002–1038. http://dx.doi.org/10.1002/fut.22317.
Zhou, Z., 1998. An equilibrium analysis of hedging with liquidity constraints, speculation, and government price subsidy in a commodity market. J. Financ. 53:5, 1705–1736. http://dx.doi.org/10.1111/0022-1082.00069.